RSC Advances

PAPER

View Article Online
View Journal | View Issue

Check for updates

Cite this: *RSC Adv.*, 2024, **14**, 9559

Dual active pyrimidine-based carbocyclic nucleoside derivatives: synthesis, and *in silico* and *in vitro* anti-diabetic and anti-microbial studies†

Kalyani Mallidi,[a] Rambabu Gundla,*[a] Parameshwar Makam,[b] Naresh Kumar Katari *[ac] and Sreekantha Babu Jonnalagadda [c]

Received 12th January 2024
Accepted 2nd March 2024

DOI: 10.1039/d4ra00304g

rsc.li/rsc-advances

Diabetes mellitus (DM) is a chronic metabolic disorder marked by high blood glucose levels, impairing glucose production in the body. Its prevalence has steadily risen over the past decades, leading to compromised immunity and heightened susceptibility to microbial infections. Immune dysfunction associated with diabetes raises vulnerability, while neuropathy dulls sensation in the extremities, reducing injury awareness. Hence, the development of novel chemical compounds for anti-diabetic and anti-infective treatments is imperative to mitigate adverse effects. In this study, we designed and synthesized pyrimidine-based carbocyclic nucleoside derivatives with C-4 substitution to assess their potential in inhibiting α-glucosidase for managing diabetes mellitus (DM) and microbial infections. Compounds **8b** and **10a** displayed promising IC50 values against α-glucosidase (43.292 nmol and 48.638 nmol, respectively) and noteworthy docking energies (−9.4 kcal mol^{-1} and −10.3 kcal mol^{-1}, respectively). Additionally, compounds **10a** and **10b** exhibited better antimicrobial activity against *Bacillus cereus*, with the zone of inhibition values of 2.2 ± 0.25 mm and 1.4 ± 0.1 mm at a 100 μl concentration, respectively. Compound **10a** also exhibited a modest zone of inhibition of 1.2 ± 0.15 mm against *Escherichia coli* at 100 μl.

Open Access Article. Published on 21 March 2024. Downloaded on 2/13/2026 12:19:14 PM.
This article is licensed under a Creative Commons Attribution-NonCommercial 3.0 Unported Licence.

1 Introduction

Diabetes Mellitus (DM) is a chronic metabolic disorder[1] characterized by elevated blood glucose levels, which impairs the body's ability to produce glucose.[2,3] Diabetes is directly accountable for causing the deaths of 1.5 million people annually. Over the past few decades, there has been a steady increase in both the occurrence and the overall number of cases of diabetes. Type 1 diabetes is caused by the autoimmune destruction of pancreatic beta cells, requiring lifelong insulin therapy,[4,5] Type 2 diabetes is caused by poor diet, lack of exercise, and obesity, leading to increased insulin resistance.[6–8] α-Glucosidase inhibitors are used to treat type 2 diabetes by slowing the absorption of carbohydrates in the small intestine.[9] These inhibitors have multiple advantages in controlling diabetes, including delayed digestion of complex carbohydrates, slowing glucose release, reducing postprandial hyperglycemia, and regulating postprandial glucose levels.[3,6] Typically used alongside other anti-diabetic medications or insulin therapy, α-glucosidase inhibitors can enhance a diabetes management plan and are rarely used as initial treatments (Fig. 1).[3,10]

Diabetes can lead to reduced immunity and increased risk of microbial infections.[11] Chronic hyperglycemia can impair neutrophil and macrophage infection defence, while wound healing is impaired due to inadequate circulation and nerve damage.[12] Elevated blood glucose levels promote the proliferation of microorganisms that facilitate the accelerated growth of pathogens such as bacteria and fungi.[13] Diabetes-related immune dysfunction increases vulnerability, and neuropathy numbs extremities, reducing awareness of injuries and wounds. Undiagnosed infections worsen, and urinary tract infections increase.[13] Diabetes-related neuropathy affects bladder function, causing incomplete emptying and infection risk. High urine glucose allows germs to grow, and diabetics with

[a]*Department of Chemistry, GITAM School of Science, GITAM Deemed to be University, Hyderabad, Telangana 502329, India. E-mail: nkatari@gitam.edu*

[b]*Department of Chemistry, School of Applied and Life Sciences, Uttaranchal University, Arcadia Grant, P.O. Chandanwari, Premnagar, Dehradun, Uttarakhand 248007, India*

[c]*School of Chemistry & Physics, College of Agriculture, Engineering & Science, WestvilleCampus, University of KwaZulu-Natal, P Bag X 54001, Durban 4000, South Africa*

† Electronic supplementary information (ESI) available. See DOI: https://doi.org/10.1039/d4ra00304g

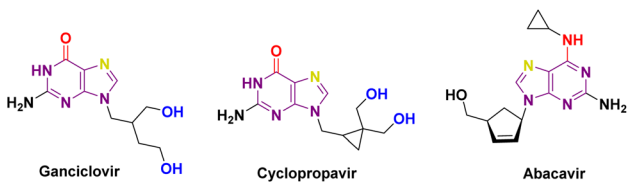

Fig. 1 Carbocyclic nucleoside analogues.

Open Access Article. Published on 21 March 2024. Downloaded on 2/13/2026 12:19:14 PM. This article is licensed under a Creative Commons Attribution-NonCommercial 3.0 Unported Licence.

retinopathy can see poorly, increasing skin and other infections.[14] High blood sugar glycates proteins and impedes infection-fighting proteins and immune cells.[15] Therefore, developing novel chemical compounds for anti-diabetic and anti-infective medications is crucial to minimize side effects. Several pharmaceutical compounds and prospective compounds categorized as carbocyclic nucleosides have been developed for the management of diabetes. Multiple studies have confirmed the importance of carbocyclic pyrimidine and purine derivatives in the field of diabetes treatment. Carbocyclic nucleoside derivatives have a wide range of applications in the treatment of numerous disorders. Various instances can be given, such as Abacavir (ABC), also referred to as Ziagen or 1592U89, which is a carbocyclic nucleoside analogue that is chemically produced from guanosine. H2G, or (R)-9-[4-hydroxy-2-(hydroxymethyl)butyl]guanine, is a type of nucleoside analogue that has shown strong effectiveness against different types of herpes viruses. Amprenavir, the fifth nonpeptidic inhibitor of HIV-1 protease to be commercially accessible, was initially created for the treatment of AIDS patients in combination with authorized antiretroviral nucleoside analogues.[16,17] Carbocyclic nucleosides have been predominantly investigated for their antiviral effects. However, they have also been examined for their ability to combat bacterial infections, particularly in the context of diabetes treatment. Diabetes mellitus increases the likelihood of different infections, such as bacterial infections, because it weakens the immune system and hampers the wound healing process.[18] Certain carbocyclic nucleosides exhibit anti-inflammatory effects, perhaps aiding in the reduction of inflammation-related problems in diabetic patients and indirectly decreasing the likelihood of bacterial infections.[19] Recent studies indicate that some carbocyclic nucleosides may demonstrate synergistic properties when used with traditional antibiotics to combat bacterial infections as well.[20]

2 Results and discussion

2.1 Design and evaluation of physico-chemical properties

Lower molecular weight and lipophilicity compounds have been shown to increase paracellular and transcellular absorption and clearance,[21–23] resulting in increased renal excretion,[24,25] and moderate toxicity.[26] The "rule of 5" (Ro5) defines a drug-like molecule (DLM). The Ro5 criterion includes molecules having a molecular mass below 500, a log P value below 5, and a hydrogen bond donor and acceptor count below 5 and 10 respectively.[27–29] According to the Veber rule, compounds with polar surface areas, hydrogen bond donors, and acceptors of 140, 10, or 12 improve oral bioavailability.[30] Leeson *et al.* found that NCEs approved from 1983 to 2002 had 16% to 23% higher molecular mass, rings, rotatable bonds, and hydrogen bonding groups. These qualities help build compounds with improved ADMET.[31–33] Physico-chemical characteristics are increasingly important in determining a molecule's therapeutic potential and efficacy during medication development (Fig. 2).[31,32]

Considering the aforementioned factors, the pyrimidine-based carbocyclic nucleoside derivatives have been achieved with diverse modifications in terms of both structure and

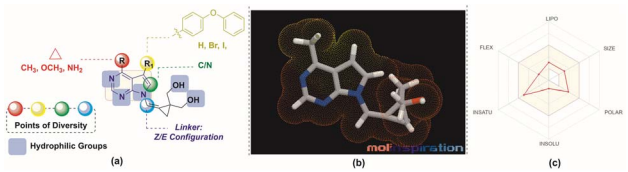

Fig. 2 (a) Design of the molecules (b) MLP 3D representation of the molecule, **8a** (c) web representation of the physico-chemical properties of the molecule, **8a**.

functionality (Table 1) (Fig. 3). The evaluation of physico-chemical and structural properties through computational methods entails the determination of various essential parameters. These parameters encompass heavy atoms (HA), heavy aromatic atoms (HAA), rotatable bonds (RB), hydrogen bond acceptors (HBA), hydrogen bond donors (HBD), molar refractivity (MR), and total polar surface area (TPSA). The SwissADME tool is employed for this purpose. The results of this analysis have been summarised in Table 1, and the observations are consistent with the established criteria for "drug-likeness" as outlined by the Lipinski, Ghose, Veber, Egan, and Muegge rules.

The pharmacokinetic characteristics of pyrimidine-based carbocyclic nucleoside derivatives, such as gastrointestinal absorption (GIA) and blood–brain–blood barrier (BBB) permeability, have also been projected. The pharmacokinetic behaviours of all pyrimidine-based carbocyclic nucleoside derivatives, including gastrointestinal absorption (GIA) and brain–blood barrier (BBB), have also been predicted. By calculating the lipophilicity (WLOGP *versus* TPSA), the Brain or IntestinaLEstimateD Permeation method (BOILEDEgg) has been visually shown (Fig. 3).[34] It is projected that all molecules fall inside the white ellipse and none fall inside the yellow ellipse and grey region. This indicates that molecules could exhibit superior GIA but poorer BBB properties. All substances whose efflux activity in the Central Nervous System (CNS) was predicted by the *P*-glycoprotein (PGP).

2.2 Synthesis of the C-4 substituted carbocyclic purine compounds (8a–8h) and (10a–10c)

The 7-deazapurine scaffold can be easily substituted with functional groups at the C-4 position by standard synthetic chemistry. Scheme 1 illustrates a seven-step general synthetic route for the preparation of **8a–8h** and **10a–10c**. The initial formation of the product was identified by MS analysis with their molecular weight. Their structures were confirmed by ^{1}H-NMR, ^{13}C NMR and FT-IR. Most of the compounds were soluble in polar solvents like DMF and DMSO. To synthesize these compounds, we have performed a de-acetylation reaction between compound 7 and commercially available LiOH·H_2O to give the corresponding compounds. The formation of C-4 substituted carbocyclic purines was confirmed by ^{1}H-NMR, ^{13}C NMR and FT-IR. In these compounds, the characteristic methoxy (–methyl) proton shifted to the downfield at δ 4.0, the pyrimidine ring proton was at around δ 8.68 and the pyrrole ring proton at 8.26 ppm (*Z*-Isomer) and proton at 7.82 ppm (*E*-

© 2024 The Author(s). Published by the Royal Society of Chemistry

Open Access Article. Published on 21 March 2024. Downloaded on 2/13/2026 12:19:14 PM.
This article is licensed under a Creative Commons Attribution-NonCommercial 3.0 Unported Licence.

Table 1 Library of pyrimidine-based carbocyclic nucleoside derivatives

Methyl Substituted 7-deazapurines					
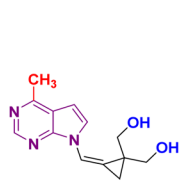	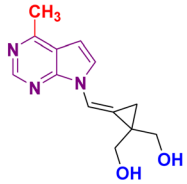	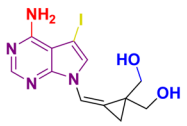	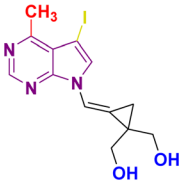	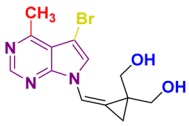	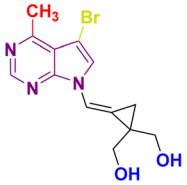
8a (*Z*-Isomer)	8a (*E*-Isomer)	8b (*Z*-Isomer)	8b (*E*-Isomer)	8c (*Z*-Isomer)	8c (*E*-Isomer)
Methoxy Substituted 7-deazapurines					
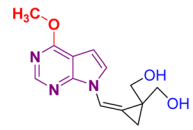	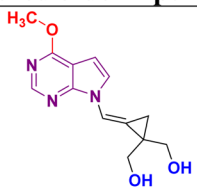	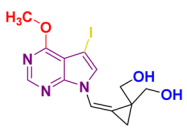	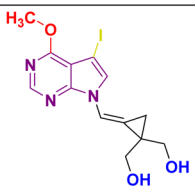		
8d (*Z*-Isomer)	8d (*E*-Isomer)	8e (*Z*-Isomer)	8e (*E*-Isomer)		
Cyclopropyl Substituted 7-deazapurines					
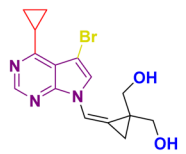	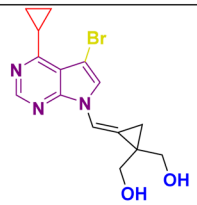				
8f (*Z*-Isomer)	8f (*E*-Isomer)				
Amino Substituted 7-deazapurines					
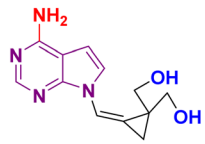	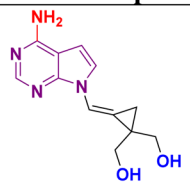	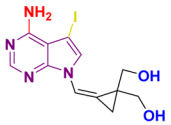	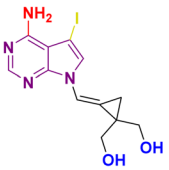		
8g (*Z*-Isomer)	8g (*E*-Isomer)	8h (*Z*-Isomer)	8h (*E*-Isomer)		
Amino Substituted 8-aza-7-deaza purine					
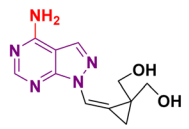	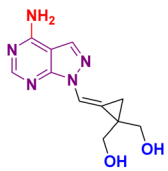	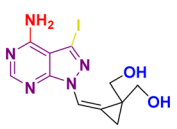	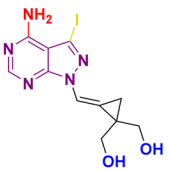	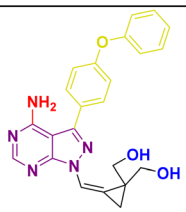	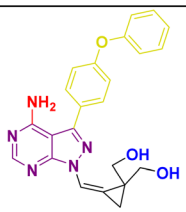
10a (*Z*-Isomer)	10a (*E*-Isomer)	10b (*Z*-Isomer)	10b (*E*-Isomer)	10c (*Z*-Isomer)	10c (*E*-Isomer)

isomer). In the ^{13}C NMR spectra, the methoxy (O–Me) appeared around δ 53.5 ppm; the cyclopropyl carbons were found in the region between δ 10.6 to 13.4 ppm. In the ^{1}H-NMR, the aromatic methoxy group protons of compound **8d** appeared at δ 4.06–4.04 ppm. In compound **8f**, the C-4 substituted cyclopropane CH proton multiplate signal was observed in *Z* and *E* isomers at δ 3.12–3.06 and 3.09–3.05 ppm. The ^{13}C NMR of NH_2 attached carbon of compounds **8g** and **8h** was shifted to downfield and appeared at δ 157.2 and the signal for carbon attached to two nitrogen pyrimidine rings was shifted to downfield and appeared at δ 152.4 respectively. The ^{13}C NMR of **8a–8h** were recorded in DMSO as an internal standard, and the signal for two hydroxyl methyl attached carbon of cyclopropane ring merged into the DMSO signal. The FT-IR data clearly defined the presence of $\nu_{(-C-X)}$ at 600–500 cm^{-1} in all compounds and $\nu_{(-NH\ for\ amino)}$ at 3501 cm^{-1} and $\nu_{(-CN\ for\ amino)}$ at 1250–1020 cm^{-1} in compound **8h**. Structural confirmation was done by NOESy1D for the **10c** (*Z*-isomer) compound.

The alcohol protected (2-bromo-2-(bromomethyl) cyclopropane-1,1-diyl)bis(methylen e) 6 was reacted with a C-4 substituted 7-deaza or 7-halo-7-deazapurines.[35,36] *N*-glycidylation reaction (**7a–7h**) followed by deacetylation to afford the desired compounds **8a–8h**. The key moiety of alcohol protected (2-bromo-2-(bromomethyl)cyclopropane-1,1-diyl)

Open Access Article. Published on 21 March 2024. Downloaded on 2/13/2026 12:19:14 PM. This article is licensed under a Creative Commons Attribution-NonCommercial 3.0 Unported Licence.

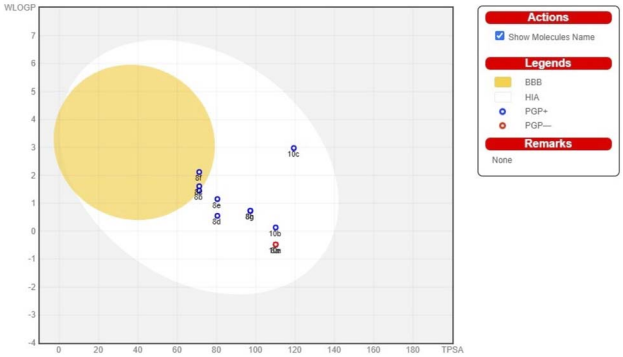

Fig. 3 BOILEDEgg of pyrimidine-based carbocyclic nucleoside derivatives.

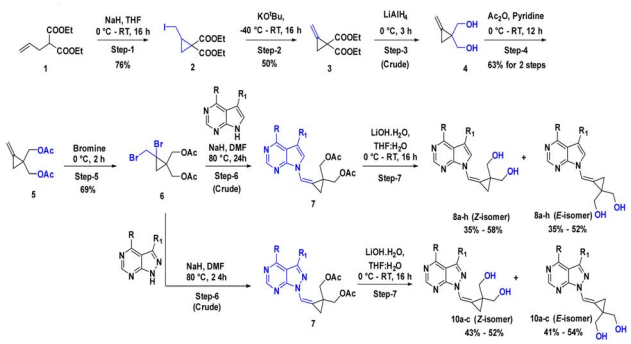

Scheme 1 Synthetic scheme for compounds **8a–8h** and **10a–10c**; Reaction conditions: step-1: NaH, I_2, THF, 0 °C RT, 16 h (Y: 76%); step-2: *t*-BuOK, THF, −40 °C RT, 16 h (Y: 50%); step-3: $LiAlH_4$, THF, 0 °C, 3 h (Y: crude); step-4: Ac_2O, pyridine, 0 °C – RT, 12 h (Y: 63% for 2 steps); step-5: Br_2, CCl_4, 0 °C, 2 h (Y: 69%); step-6: NaH, DMF, 80 °C, 24 h (Y: crude); step-7: $LiOH{\cdot}H_2O$, THF: H_2O, 0 °C RT, 16 h (Y: 35–55% for 2 steps to all compounds).

bis(methylene) compound 6 was prepared using the diethyl 2-allylmalonate as a starting material, which on treatment with NaH and Iodination with I_2 gave diethyl 2-(iodomethyl) cyclopropane-1,1-dicarboxylate moiety. This compound on double bond formation with KO^{t}Bu resulted in diethyl 2-methylenecyclopropane-1,1-dicarboxylate compound **3**. Compound **3** was reduced with $LiAlH_4$ reagent resulting in the intermediate **4**.[37] The compound **4** (ref. 38 and 39) in the presence of acetic anhydride and pyridine resulted in intermediate **5**. Bromination with bromine gave the key intermediate **6** (ref. 40 and 41), with this intermediate conducted *N*-glycidylation reaction with different C-4 substituted 7-deaza or 7-halo-7-deazapurines resulted in their respective products **7a–7h** in 65–70% yield. Further, deprotection with $LiOH{\cdot}H_2O$ gave the first set of our target molecules **8a–8h** (Table 1). The structures of the final compounds **8a–8h** were confirmed by spectral characterization data using ^{1}H-NMR, ^{13}C-NMR, MS, and FT-IR (ESI†). ^{1}H-NMR of compound **8a** indicated singlet at δ 8.69 ppm for Pyrimidine ring proton (proton between nitrogen's), the doublet with chemical shift value of δ 8.37–8.36 ppm for pyrrole ring proton (proton adjacent to NH) and 7.68 ppm for alkene proton and the olefin proton was seen in the downfield region of δ 7.68 ppm. The ^{13}C NMR spectra showed C-4 substituted methyl carbon shifted upfield at δ 21.1 and C7 position carbon shifted at δ 101.1 and δ 111.6 for alkene carbon. MS (ESI): $m/z = 246.5$ $(M + H)^+$. The ^{13}C signal for two hydroxyl methyl attached carbon of cyclopropane ring merged into the DMSO signal. The FT-IR data clearly defined the presence of $\nu_{(-C-O \text{ for alcohol})}$ and $\nu_{(-C=C \text{ for alkene})}$ at 1029 and 1564 cm^{-1}, respectively.

To synthesize compounds **10a–c**, the key building block intermediate, **6(b)** was used along with C-4 substituted 8-aza-7-deaza purines[42,43] and the same protocol was followed and afford target compounds **10a–c** (Table 1) (Scheme 1). In the ^{1}H-NMR spectrum of all the new compounds synthesized from intermediate, **6(b)**, the characteristic 7-deaza (–CH–) proton signal was observed at δ 8.22 ppm. The two doublets were observed δ 3.65 and 3.52 ppm and one broad singlet was observed for hydroxy at 4.87 ppm. cyclopropyl ring protons ranged at δ 1.40 ppm. Moreover, the broad singlet for pyrimidine ring proton was observed around δ 8.22 ppm. The ^{13}C signal was noticed at δ 116.5 ppm for 7-deaza carbon, and the ^{13}C signal for two hydroxyl methyl attached carbon of cyclopropane ring merged into the DMSO signal, respectively. MS (ESI): $m/z = 248.5$ $(M + H)^+$. In FT-IR, a strong band for $\nu_{(C-O)}$ around 1035 cm^{-1}, $\nu_{(-C-O \text{ for primary alcohol})}$ 3564 cm^{-1} was seen δ 1.44 and 4.88 ppm was correlation was observed on **10c** (*Z*-Isomer) by NOESy1D.

2.3 Docking studies

Molecular docking was performed on the synthesized compounds. Further, screening was done using AutoDock Vina for precision (Fig. 4). Among the screened compounds, the compound with the highest docking energy was found to be with **10a** (*E*-Isomer) and **8b** (*E*-Isomer), whereas the compound with the lowest docking energy was **8c** (*E*-Isomer). The compound **10a** (*E*-Isomer) demonstrated a docking energy of −10.3 kcal mol^{-1}. The presence of conventional hydrogen bonding with Gln279, Arg442, Glu277, Asp215, and Arg213 is evident, along with a carbon–hydrogen bond with Asp352. Subsequently, compound **8b** (*E*-Isomer) exhibited the second-highest docking energy of −9.7 kcal mol^{-1}. The presence of conventional hydrogen bonds with Asp69 and Arg442 was observed. Compound **8c** (*Z*-Isomer) had the lowest docking energy, with a value of −7.1 kcal mol^{-1}. Conventional hydrogen bonds with Asp215 and carbon–hydrogen bonds with Asp352 were observed (ESI Table 1†).

2.4 Inhibition of α-glucosidase by C-4 substituted carbocyclic purine compounds

To assess the efficacy of the synthesized derivatives in treating diabetes, an investigation was conducted to determine the inhibitory capability of these compounds against α-glucosidase. The results of this investigation are presented in the table. Acarbose was employed as a positive control, exhibiting an IC_{50} value of 35.91 nmol. Two compounds, namely **8b** (*E*-Isomer) and

© 2024 The Author(s). Published by the Royal Society of Chemistry

Open Access Article. Published on 21 March 2024. Downloaded on 2/13/2026 12:19:14 PM.
This article is licensed under a Creative Commons Attribution-NonCommercial 3.0 Unported Licence.

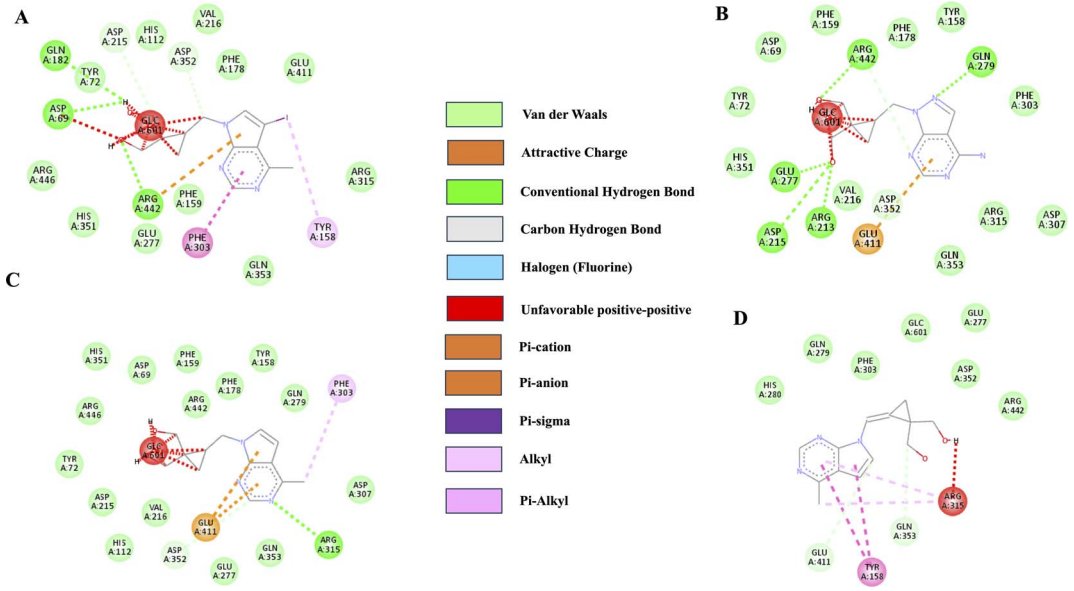

Fig. 4 2D Ligand interaction diagrams for docking-compound: (A)**8b** (*E*-Isomer), (B) **10a** (*E*-Isomer), (C) **8c** (*Z*-Isomer) and (D) **8a** (*Z*-Isomer) against α-glucosidase (3A4B.PDBID).

10a (*E*-Isomer), exhibited favourable IC_{50} values of 43.292 nmol and 48.638 nmol, respectively. The compounds with relatively low IC_{50} values were identified as **8f** (*E*-Isomer) and **8c** (*E*-Isomer) with IC_{50} values of 91.714 nmol and 100.16 nmol, respectively (ESI Table 2†).

2.5 Antimicrobial activity

2.5.1. Antibacterial activity. The synthesized molecules were evaluated for their antibacterial activity against four bacterial strains that included two Gram-positive bacteria *Bacillus cereus* and *Staphylococcus* and two Gram-negative bacteria *Escherichia coli* and *Klebsiella*. Ciprofloxacin was used as a positive reference (ESI Fig. 2†). The concentration of the compounds used was 1 mg mL^{-1}. The zone of inhibition was determined and tabulated. According to the results, none of the compounds were effective against *Staphylococcus* (Gram-positive) and *Klebsiella* (Gram-negative) (ESI Table 2†). The compounds failed to show any zone of inhibition for these organisms on the Mueller–Hinton agar plates. When tested against the Gram-positive bacteria *Bacillus cereus*, it was observed that compounds **10a** (*E*-Isomer), **10b** (*Z*-Isomer and *E*-Isomer), **10c** (*Z*-Isomer and *E*-Isomer), showed inhibitory activity. Maximum inhibition was observed using the compound **10b** (*Z*-Isomer) (2.2 ± 0.25 mm) at 100 μl. For the Gram-negative *Escherichia coli*, the zone of inhibition was observed using compound **10a** (*E*-Isomer) only. The radius of the inhibition was observed at 75 μl (0.9 ± 0.05 mm) and 100 μl (1.2+/0.15 mm) (ESI Fig. 1A†).

2.5.2. Antifungal activity. The effectiveness of the synthesized compounds as antifungal drugs was studied using *Aspergillus niger*. None of the synthesized derivatives showed any effect on its growth as shown in ESI Fig. 1B.† Upon conducting tests to evaluate the anti-fungal activity, it was observed that the synthesized compounds did not exhibit any inhibitory effects against *Aspergillus niger* using fluconazole as a control (ESI Fig. 3†).

In a recent research, Nguyen *et al.* conducted a study on the α-glucosidase inhibitory and antimicrobial properties of benzoyl phloroglucinols derived from the fruit of *Garcinia schomburgkiana*.[44] The results of the antimicrobial assessment demonstrated that a newly discovered polyprenylated benzoyl phloroglucinol, referred to as *schomburgkianone* I (compound **1**), as well as a previously identified compound known as *guttiferone* K (compound **2**), exhibited inhibitory effects on *Staphylococcus* and *Enterococcus faecium* at the concentration tested. However, no activity against *Acinetobacter baumannii* was observed.[44] In their study, Kaur *et al.* assessed the antibacterial and anti-biofilm properties of alpha-glucosidase inhibitors derived from the endophytic fungus *Alternaria destruens*. The efficacy of active fractions AF1 and AF2 derived from *Aspergillus destruens* was assessed against various bacterial strains including *Salmonella enterica*, *Shigella flexneri*, *Vibrio cholerae*, *Escherichia coli*, *Pseudomonas aeruginosa*, *Staphylococcus aureus*, and *Candida albicans*. The study demonstrated that AF1 had antibacterial properties against all the pathogens that were examined. In contrast, AF2 only exhibited antibacterial activity against specific pathogens, including *Staphylococcus aureus*, *Vibrio cholerae*, *Salmonella enterica*, and *Candida albicans*.[40]

Our findings suggested that among the synthesized compounds, **8bn** (*E*-Isomer) and **10a** (*E*-Isomer), exhibited favourable IC_{50} values of 43.292 nmol and 48.638 nmol, respectively. The positive control Acarbose has an IC_{50} value of 35.91 nmol. The IC_{50} value is associated with drug potency, *i.e.*, the amount of drug necessary to induce the effect, the lower the IC_{50} value, the more effective the drug.[45] Acarbose exhibits a better inhibitory effect against the enzyme α-glucosidase than the produced chemicals. However, in comparison to the

Open Access Article. Published on 21 March 2024. Downloaded on 2/13/2026 12:19:14 PM. This article is licensed under a Creative Commons Attribution-NonCommercial 3.0 Unported Licence.

derivative **8c** (*E*-Isomer), with an IC_{50} value of 100.16 nmol, compounds **8b** (*E*-Isomer), and **10a** (*E*-Isomer), are more active, comparatively. Results of docking also showed that the compounds **8b** (*E*-Isomer) and **10a** (*E*-Isomer), showed good docking scores of −9.4 kcal mol^{-1} and −10.3 kcal mol^{-1}, respectively.

New α-glucosidase inhibitors are always being explored. In a study, the alpha-glucosidase inhibitor action of novel N-substituted 5-benzylidene-2,4-thiazolidinedione derivatives were performed. All substances demonstrated various degrees of α-glucosidase inhibitory activity as compared to acarbose. When compared to acarbose (IC_{50} = 67.06 ± 1.24 μM), most compounds displayed extremely considerable inhibitory activity towards α-glucosidase.[46] Flavonoids are known to play a function in hypoglycemia *via* blocking α-glucosidase. A study indicated that the diverse flavonoid compounds exhibited inhibitory activity and good docking score and the presence of Asp 215 was implicated in the hydrogen-bonding interaction between each flavonoid with the enzyme. Also, hydrophobic interactions with Tyr 72, Tyr 158, Phe 159, Phe 178, Asp 352, and Arg 442 were found. These amino acids are recurrent in our synthesized compounds as well.

3 Experimental section

3.1 Chemicals and reagents

All chemicals (reagent grade) used were purchased from Combi-Blocks (USA), Johnson Matthey Co., Ltd (USA) and Enamine Ltd (Ukraine). All the solvents used for the reaction are LR grade. Analytical thin-layer chromatography (TLC) was performed on pre-coated silica gel $60F_{254}$ plates, and visualization of TLC was achieved by UV light. Flash column chromatography was undertaken on silica gel (100–200 mesh). ^{1}H NMR was recorded at 400 or 500 MHz, and chemical shifts were quoted in parts per million (ppm) referenced to 0.0 ppm for tetramethyl silane. The following abbreviations were used to describe peak splitting patterns when appropriate: br = broad, s = singlet, d = doublet, t = triplet, q = quartet, m = multiplet, dd = doublet of doublet. Coupling constants, *J*, were reported in the hertz unit (Hz). ESI mass spectra were obtained on Agilent and Waters instruments. All the final compounds were purified on GRACE flash chromatography by using C18 reverse-phase columns. The mobile phase was a mixture of water (0.1% formic acid) and acetonitrile. Melting points were recorded on the Buchi M − 560 instrument.

3.2 Chemistry

3.2.1. Synthesis of compound 8a. To a solution of intermediate **6** (1.0 eq.) in DMF (10 mL) at room temperature, NaH (2.0 eq.), 4-methyl-7*H*-pyrrolo[2,3-*d*] pyrimidine (1.2 eq.) were added and the resulting reaction mixture was maintained under stirring at 80 °C for 24 h. The reaction mixture was allowed to room temperature, diluted with ethyl acetate (25–30 mL), added 0.2 g of activated charcoal, and filtered through the celite. The filtrate was partitioned between water and ethyl acetate. The combined ethyl acetate layer was washed with brine, dried over anhydrous Na_2SO_4 and concentrated to afford crude reaction mass (2-((4-methyl-7*H*-pyrrolo[2,3-*d*] pyrimidin-7-yl) methylene) cyclopropane-1,1-diyl) bis(methylene) diacetate as a pale-yellow oil. The crude proceeded to the next step without any further purification. This crude was dissolved in THF : H_2O (7 : 3 ratio, 10 mL) at 0 °C, $LiOH \cdot H_2O$ (1.5 eq.) was added and the reaction mixture was stirred at room temperature for 16 h. The reaction mixture was partitioned between water (30 mL) and DCM (30 mL × 3). The combined organic layer was washed with water (30 mL), and brine (30 mL), dried over anhydrous Na_2SO_4 and concentrated. The crude was purified by GRACE flash chromatography using a C18 column with water and acetonitrile as an eluent to give the final compound (Z)-(2-((4-methyl-7*H*-pyrrolo [2,3-*d*]pyrimidin-7-yl)methylene)cyclopropane-1,1-diyl) dimethanol **8a** (*Z*-Isomer) as an off-white solid (125 mg, 42% Yield for 2 steps) and (*E*)-(2-((4-methyl-7*H*-pyrrolo[2,3-*d*] pyrimidin-7-yl)methylene)cyclopropane-1,1-diyl)dimethanol (**8a**-*E*-Isomer) as an off-white solid (105 mg, 40% yield for 2 steps).

8a (*Z*-Isomer): ^{1}H-NMR (400 MHz, DMSO-d_6) δ 1.22 (s, 2H, Cyclopropyl CH_2, shielding proton), 2.66 (s, 3H), 3.56–3.54 (d, 2H, J = 7.6 Hz, –C(C***H***$_2$)), 3.66–3.64 (d, 2H, J = 10 Hz, –C(C***H***$_2$)), 5.08 (brs, 2H, O***H***), 6.83 (d, 1H, J = 2.8 Hz, Ar–***H***), 7.68 (brs, 1H), 8.37–8.36 (d, 1H, J = 2.8 Hz, Ar–***H***), 8.69 (brs, 1H, Ar–*H*). ^{13}C NMR (400 MHz, DMSO-d_6), δ 10.74 (cyclo propyl carbon), 21.14, 30.49, 39.90 (–C attached to hydroxyl methyl) (merged in DMSO moisture),43.85(–***C***$(CH_2)_2$), 62.30 (–***C***$(CH_2)_2$), 101.10 (–*C*7, pyrrole ring),111.67, 114.76, 117.53, 125.44 (-*C*═*C*), and 148.45, 151.25, 159.048 (Ar–***C***). MS (ESI): m/z = 246.5 $(M + H)^+$.

8a (*E*-Isomer): FT-IR (KBr): $\nu_{(-O-H)}$: 3363 cm^{-1}; $\nu_{(-C-O)}$: 1029 cm^{-1}; $\nu_{(-C-C \text{ for aromatic ring})}$: 1564 cm^{-1}; $\nu_{(-C-N)}$: 1325 cm^{-1}. ^{1}H-NMR (400 MHz, DMSO-d_6) δ 1.54 (s, 2H, cyclopropyl CH_2, deshielding proton), 2.66 (s, 3H), 3.54–3.51 (m, 4H, –C(C***H***$_2$)), 4.78 (brs, 2H, O***H***), 6.88–6.87 (d, 1H, J = 3.6 Hz, Ar–***H***), 7.80 (brs, 1H), 7.95–7.94 (d, 1H, J = 3.6 Hz, Ar–***H***), 8.69 (brs, 1H, Ar–*H*). ^{13}C NMR (400 MHz, DMSO-d_6), δ 13.45 (Cyclo propyl Carbon), 21.17, 28.19, 39.70 (–C attached to hydroxyl methyl) (merged in DMSO moisture), 62.58 (–***C***$(CH_2)_2$), 101.32 (–*C*7, pyrrole ring),111.30, 115.16, 117.41, 124.47 (–*C*═*C*), and 148.62, 151.32, 159.23 (Ar–***C***). MS (ESI): m/z = 246.5 $(M + H)^+$.

3.2.2. (2-((5-Iodo-4-methyl-7*H*-pyrrolo[2,3-*d*] pyrimidin-7-yl)methylene)cyclopropane-1,1-diyl) dimethanol (8b): compound 8b was obtained from (2-bromo-2-(bromomethyl) cyclopropane-1,1-diyl) bis(methylene) diacetate followed by deacetylation. *Z*-Isomer is a pale brown solid and *E*-Isomer is a brown solid. 8b (*Z*-Isomer): Yield: 140 mg (40%). FT-IR (KBr): $\nu_{(-O-H)}$: 3324 cm^{-1}; $\nu_{(-C-O)}$: 1025 cm^{-1}; $\nu_{(-C-C \text{ for aromatic ring})}$: 1555 cm^{-1}; $\nu_{(-C-N)}$: 1335 cm^{-1}, $\nu_{(-C-I)}$: 567 cm^{-1}. ^{1}H-NMR (400 MHz, DMSO-d_6) δ 1.58 (s, 2H, cyclopropyl CH_2), 2.90 (s, 3H), 3.54–3.51 (q, J = 11.2 Hz, 4H, –C(C***H***$_2$)), 4.75 (brs, 2H, O***H***), 7.75 (s, 1H), 8.11 (s, 1H, Ar–***H***), 8.71 (s, 1H, Ar–*H*). ^{13}C NMR (400 MHz, DMSO-d_6), δ 13.53, 20.50, 28.23, 39.91 (–C attached to hydroxyl methyl) (merged in DMSO moisture), 55.65 (halo substituted carbon, pyrrole ring), 62.50 (–***C***$(CH_2)_2$), 110.60, 116.31, 117.47, 129.41(–*C*═*C*), and 148.18, 151.38, 159.77 (Ar–***C***). MS (ESI): m/z = 372.4 $(M + H)^+$.

© 2024 The Author(s). Published by the Royal Society of Chemistry

Open Access Article. Published on 21 March 2024. Downloaded on 2/13/2026 12:19:14 PM. This article is licensed under a Creative Commons Attribution-NonCommercial 3.0 Unported Licence.

8b (*E*-Isomer): Yield: 130 mg (35%). ^{1}H-NMR (400 MHz, DMSO-d_6) δ 1.32 (s, 2H, cyclopropyl CH_2), 2.88 (s, 3H), 3.53–3.50 (d, J = 12.0 Hz, 2H, (C***H***$_2$)), 3.68–3.66 (d, J = 8.0 Hz, 2H, (C***H***$_2$)), 5.09 (brs, 2H, O***H***), 7.63 (brs, 1H), 8.67 (s, 1H, Ar–***H***), 8.70 (s, 1H, Ar–*H*). ^{13}C NMR (400 MHz, DMSO-d_6), δ 10.78, 20.44, 30.49, 39.91 (–C attached to hydroxyl methyl) (merged in DMSO moisture), 55.29 (halo substituted carbon, pyrrole ring), 62.22 (–***C***$(CH_2)_2$), 110.05, 115.64, 117.51, 130.79 (–*C*═*C*), and 148.02, 151.31, 159.58 (Ar–***C***). MS (ESI): m/z = 372.4 (M + H)$^+$.

3.2.3. (2-((5-Bromo-4-methyl-7*H*-pyrrolo[2,3-*d*] pyrimidin-7-yl) methylene) cyclopropane-1,1-diyl) dimethanol (8c): compound 8c was obtained from (2-bromo-2-(bromomethyl) cyclopropane-1,1-diyl) bis(methylene) diacetate fallowed by deacetylation. *Z*-Isomer is a pale yellow solid and *E*-Isomer is a pale-yellow solid. 8c (*Z*-Isomer): Yield: 130 mg (36%). FT-IR (KBr): $\nu_{(-O-H)}$: 3322 cm^{-1}; $\nu_{(-C-O)}$:1026 cm^{-1}; $\nu_{(-C-C\ for\ aromatic\ ring)}$: 1556 cm^{-1}; $\nu_{(-C-N)}$: 1342 cm^{-1}, $\nu_{(-C-Br)}$: 604 cm^{-1}. ^{1}H-NMR (400 MHz, DMSO-d_6) δ 1.58 (s, 2H, cyclopropyl CH_2), 2.86 (s, 3H), 3.54–3.43 (m, 4H, –C(C***H***$_2$)), 4.78–4.76 (t, J = 8.0 Hz,2H, O***H***), 7.78 (s, 1H), 8.12 (s, 1H, Ar–***H***), 8.74 (s, 1H, Ar–*H*). ^{13}C NMR (400 MHz, DMSO-d_6), δ 13.58, 20.95, 28.31, 39.91 (-C attached to hydroxyl methyl) (merged in DMSO moisture), 62.52 (–***C***$(CH_2)_2$), 89.63 (halo substituted carbon, pyrrole ring), 110.63, 115.14, 116.53, 124.41 (–*C*═*C*), and 147.71, 151.89, 159.59 (Ar–***C***). MS (ESI): m/z = 324.5 (M + H)$^+$.

8c (*Z*-Isomer): Yield: 130 mg (36%). FT-IR (KBr): $\nu_{(-O-H)}$: 3098 cm^{-1}; $\nu_{(-C-O)}$:1032 cm^{-1}; $\nu_{(-C-C\ for\ aromatic\ ring)}$: 1562 cm^{-1}; $\nu_{(-C-N)}$: 1342 cm^{-1}, $\nu_{(-C-Br)}$: 604 cm^{-1}. ^{1}H-NMR (400 MHz, DMSO-d_6) δ 1.33 (s, 2H, cyclopropyl CH_2), 2.85 (s, 3H), 3.53–3.49 (m, 2H, (C***H***$_2$)), 3.70–3.66 (m, 2H, (C***H***$_2$)), 5.09 (brs, 2H, O***H***), 7.67 (brs, 1H), 8.65 (s, 1H, Ar–***H***), 8.73 (s, 1H, Ar–*H*). MS (ESI): m/z = 324.5 (M + H)$^+$.

3.2.4. (2-((4-methoxy-7*H*-pyrrolo[2,3-*d*] pyrimidin-7-yl) methylene) cyclopropane-1,1-diyl) dimethanol (8d): compound 8d was obtained from (2-bromo-2-(bromomethyl) cyclopropane-1,1-diyl) bis(methylene) diacetate fallowed by deacetylation. *Z*-Isomer is a pale brown solid and *E*-Isomer is a brown solid. 8d (*Z*-Isomer): Yield: 120 mg (41%). ^{1}H-NMR (400 MHz, DMSO-d_6) δ 1.28 (s, 2H, cyclopropyl CH_2), 3.57–3.54 (d, J = 12 Hz, 2H), 3.67–3.66 (d, J = 12 Hz, 2H, –C(C***H***$_2$)), 4.04 (s, 3H), 5.04 (brs, 2H, O***H***), 6.67–6.66 (d, J = 4.0 Hz, 1H), 7.66 (s, 1H), 8.27–8.26 (d, J = 4.0 Hz, 1H, Ar–***H***), 8.47 (s, 1H, Ar–*H*). ^{13}C NMR (400 MHz, DMSO-d_6), δ 10.60, 30.49, 39.92 (–C attached to hydroxyl methyl) (merged in DMSO moisture), 53.55, 62.30 (–***C***$(CH_2)_2$), 99.70, 104.75, 112.00, 114.75, 123.82 (–*C*═*C*), and 150.17, 151.06, 162.30 (Ar–***C***). MS (ESI): m/z = 262.5 (M + H)$^+$.

8d (*E*-Isomer): Yield: 105 mg (36%). FT-IR (KBr): $\nu_{(-O-H)}$: 3327 cm^{-1}; $\nu_{(-C-O)}$:1010 cm^{-1}; $\nu_{(-C-C\ for\ aromatic\ ring)}$: 1562 cm^{-1}; $\nu_{(-C-N)}$: 1310 cm^{-1}. ^{1}H-NMR (400 MHz, DMSO-d_6) δ 1.53 (s, 2H, cyclopropyl CH_2), 3.54–3.46 (m, 4H, (C***H***$_2$)), 4.06 (s, 3H), 4.74 (brs, 2H, O***H***), 6.70–6.69 (d, J = 4.0 Hz, 1H), 7.79 (s, 1H), 7.83–7.82 (d, J = 4.0 Hz, 1H, Ar–***H***), 8.49 (s, 1H, Ar–*H*). MS (ESI): m/z = 262.5 (M + H)$^+$. ^{13}C NMR (400 MHz, DMSO-d_6), δ 13.41, 28.17, 39.92 (–C attached to hydroxyl methyl) (merged in DMSO moisture), 53.58, 62.58 (–***C***$(CH_2)_2$), 99.88, 104.66, 111.61, 115.23, 122.83 (–*C*═*C*), and 150.31, 151.14, 162.33 (Ar–***C***). MS (ESI): m/z = 262.5 (M + H)$^+$.

3.2.5. (2-((5-iodo-4-methoxy-7*H*-pyrrolo[2,3-*d*] pyrimidin-7-yl) methylene) cyclopropane-1,1-diyl) dimethanol (8e): compound 8e was obtained from (2-bromo-2-(bromomethyl) cyclopropane-1,1-diyl) bis(methylene) diacetate fallowed by deacetylation. *Z*-Isomer is a white solid and *E*-Isomer is an off-white solid. 8e (*Z*-Isomer): Yield: 150 mg (35%). ^{1}H-NMR (400 MHz, DMSO-d_6) δ 1.26 (s, 2H, cyclopropyl CH_2), 4.06 (s, 3H), 3.54–3.51 (q, J = 11.2 Hz, 4H, –C(C***H***$_2$)), 4.75 (brs, 2H, O***H***), 7.75 (s, 1H), 8.11 (s, 1H, Ar–***H***), 8.71 (s, 1H, Ar–*H*). ^{13}C NMR (400 MHz, DMSO-d_6), δ 13.53, 30.49, 39.91 (–C attached to hydroxyl methyl) (merged in DMSO moisture), 55.65 (halo substituted carbon, pyrrole ring), 53.58, 62.50 (–***C***$(CH_2)_2$), 110.60, 116.31, 117.47, 129.41 (–*C*═*C*), and 148.18, 151.38, 159.77 (Ar–***C***). MS (ESI): m/z = 388.0 (M + H)$^+$.

8e (*E*-Isomer): Yield: 150 mg (35%). FT-IR (KBr): $\nu_{(-O-H)}$: 3327 cm^{-1}; $\nu_{(-C-O)}$:1010 cm^{-1}; $\nu_{(-C-C\ for\ aromatic\ ring)}$: 1562 cm^{-1}; $\nu_{(-C-N)}$: 1310 cm^{-1}, $\nu_{(-C-I)}$: 567 cm^{-1}. ^{1}H-NMR (400 MHz, DMSO-d_6) δ 1.53 (s, 2H, cyclopropyl CH_2), 3.54–3.46 (m, 4H, (C***H***$_2$)), 4.06 (s, 3H), 4.74 (brs, 2H, O***H***), 6.70–6.69 (d, J = 4.0 Hz, 1H), 7.79 (s, 1H), 7.83–7.82 (d, J = 4.0 Hz, 1H, Ar–***H***), 8.49 (s, 1H, Ar–*H*). MS (ESI): m/z = 262.5 (M + H)$^+$. ^{13}C NMR (400 MHz, DMSO-d_6), δ 13.41, 28.17, 39.92 (–C attached to hydroxyl methyl) (merged in DMSO moisture), 55.62 (halo substituted carbon, pyrrole ring), 53.58, 62.58 (–***C***$(CH_2)_2$), 99.88, 104.66, 111.61, 115.23, 122.83 (–*C*═*C*), and 150.31, 151.14, 162.33 (Ar–***C***). MS (ESI): m/z = 388.0 (M + H)$^+$.

3.2.6. (2-((5-bromo-4-cyclopropyl-7*H*-pyrrolo[2,3-*d*] pyrimidin-7-yl) methylene) cyclopropane-1,1-diyl) dimethanol (8f): compound 8f was obtained from (2-bromo-2-(bromomethyl) cyclopropane-1,1-diyl) bis(methylene) diacetate followed by deacetylation. *Z*-Isomer is an off-white solid and *E*-Isomer is an off-white solid. 8f (*E*-Isomer): Yield: 180 mg (46%). ^{1}H-NMR (400 MHz, DMSO-d_6) δ 1.25–1.18 (m, 4H), 1.59–1.58 (d, J = 4.0 Hz, 2H, cyclopropyl CH_2), 3.12–3.06 (m, 1H), 3.54–3.44 (m, 4H, –C(C***H***$_2$)), 4.76–4.75 (t, J = 4.0 Hz, 2H, O***H***), 7.77 (s, 1H), 8.12 (s, 1H, Ar–***H***), 8.68 (s, 1H, Ar–*H*). ^{13}C NMR (400 MHz, DMSO-d_6), δ 13.54, 28.25, 39.91 (–C attached to hydroxyl methyl) (merged in DMSO moisture), 62.48 (–***C***$(CH_2)_2$), 79.17, 89.14, 110.60, 114.48, 116.37, 124.42 (–*C*═*C*), and 147.48, 152.14, 164.37 (Ar–***C***). MS (ESI): m/z = 350.5 (M + H)$^+$.

8f (*Z*-Isomer): Yield: 170 mg (43%). FT-IR (KBr): $\nu_{(-O-H)}$: 3273 cm^{-1}; $\nu_{(-C-O)}$: 984 cm^{-1}; $\nu_{(-O-C)}$: 1039 cm^{-1}; $\nu_{(-C-C\ for\ aromatic\ ring)}$: 1556 cm^{-1}; $\nu_{(-C-N)}$: 1338 cm^{-1}, $\nu_{(-C-Br)}$: 597 cm^{-1}. ^{1}H-NMR (400 MHz, DMSO-d_6) δ 1.26–1.17 (m, 4H, Cyclo propyl CH_2), 1.32 (s, 2H, cyclopropyl CH_2), 3.09–3.05 (m, 1H, cyclopropyl CH), 3.54–3.49 (m, 2H (C***H***$_2$)), 3.70–3.66 (m, 2H, (C***H***$_2$)), 5.09–5.07 (t, J = 8.0 Hz, 2H), 7.66 (brs, 1H), 8.64 (s, 1H, Ar–***H***), 8.67 (s, 1H, Ar–*H*). MS (ESI): m/z = 262.5 (M + H)$^+$. ^{13}C NMR (400 MHz, DMSO-d_6), δ 12.19, 30.48, 39.92 (–C attached to hydroxyl methyl) (merged in DMSO moisture), 62.23 (–***C***$(CH_2)_2$), 88.85, 111.07, 114.53, 115.63, 125.45 (–*C*═*C*), and 147.30, 152.05, 164.15 (Ar–***C***). MS (ESI): m/z = 350.5 (M + H)$^+$.

3.2.7. (2-((4-amino-7*H*-pyrrolo[2,3-*d*] pyrimidin-7-yl) methylene)cyclopropane-1,1-diyl)dimethanol (8g): compound 8g was obtained from (2-bromo-2-(bromomethyl)cyclopropane-1,1-diyl)bis(methylene)diacetate followed by deacetylation. *Z*-

Open Access Article. Published on 21 March 2024. Downloaded on 2/13/2026 12:19:14 PM. This article is licensed under a Creative Commons Attribution-NonCommercial 3.0 Unported Licence.

Isomer is a brown solid and *E*-Isomer is a pale brown solid. 8g (*Z*-Isomer): Yield: 160 mg (58%). ^{1}H-NMR (400 MHz, DMSO-d_6) δ 1.38 (s, 2H, cyclopropyl CH_2), 3.12–3.06 (m, 1H), 3.52–3.45 (m, 2H, –C(CH_2)), 3.66–3.6 (m, 2H, –C(C***H***$_2$)), 5.03–5.02 (t, J = 4.0 Hz, 2H, O***H***), 6.72 (br, 2H, amine proton), 7.52 (s, 1H), 8.14 (s, 1H, Ar–***H***), 8.29 (s, 1H, Ar–*H*). ^{13}C NMR (400 MHz, DMSO-d_6), δ 10.70, 30.40, 39.91 (–C attached to hydroxyl methyl) (merged in DMSO moisture), 62.30 (–***C***(CH_2)$_2$), 98.23 (C7 carbon), 102.87, 111.54, 114.48, 126.23 (–*C*═*C*), and 148.49, 152.42, 157.21 (Ar–***C***). MS (ESI): m/z = 247.1 (M + H)$^+$.

8g (*E*-Isomer): Yield: 145 mg (52%). FT-IR (KBr): $\nu_{(-O-H)}$: 3273 cm^{-1}; $\nu_{(-C-O)}$: 984 cm^{-1}; $\nu_{(-O-C)}$: 1039 cm^{-1}; $\nu_{(-C-C \text{ for aromatic ring})}$: 1556 cm^{-1}; $\nu_{(-C-N)}$: 1338 cm^{-1}, $\nu_{(-C-Br)}$: 597 cm^{-1}. ^{1}H-NMR (400 MHz, DMSO-d_6) δ 1.52 (s, 2H, cyclopropyl CH_2), 3.50–3.43 (m, 4H (C***H***$_2$)$_2$), 4.71 (s, 2H), 6.76 (brs, 2H), 7.64 (brs, 1H), 7.77 (s, 1H, Ar–***H***), 8.15 (s, 1H, Ar–*H*). ^{13}C NMR (400 MHz, DMSO-d_6), δ 13.45, 28.07, 39.92 (–C attached to hydroxyl methyl) (merged in DMSO moisture), 62.56 (–***C***(CH_2)$_2$), 98.23 (C7 carbon), 102.86, 111.04, 115.00, 125.78 (–*C*═*C*), and 148.65, 152.48, 157.26 (Ar–***C***). MS (ESI): m/z = 247.1 (M + H)$^+$.

3.2.8. (2-((4-amino-5-iodo-7*H*-pyrrolo[2,3-*d*] pyrimidin-7-yl) methylene)cyclopropane-1,1-diyl)dimethanol (8h): compound 8h was obtained from (2-bromo-2-(bromomethyl)cyclopropane-1,1-diyl)bis(methylene)diacetate followed by deacetylation. *Z*-Isomer is a pale yellow solid and *E*-Isomer is a yellow solid. 8h (*Z*-Isomer): Yield: 180 mg (43%). FT-IR (KBr): $\nu_{(-O-H)}$: 3232 cm^{-1}; $\nu_{(-N-H \text{ bending})}$: 1633 cm^{-1}; $\nu_{(-C=C, \text{ aromatic})}$: 1565 cm^{-1}; $\nu_{(-C-O)}$: 984 cm^{-1}; $\nu_{(-O-C)}$: 1021 cm^{-1}; $\nu_{(-C-N)}$: 1270 cm^{-1}, $\nu_{(-C-I)}$: 647 cm^{-1}. ^{1}H-NMR (400 MHz, DMSO-d_6) δ 1.43 (s, 2H, cyclopropyl CH_2), 3.49–3.47 (d, J = 2H, –C(CH_2)), 3.68–3.65 (d, J = 12 HZ, 2H, –C(C***H***$_2$)), 4.70 (s 2H, O***H***), 6.72 (br, 1H, amine proton), 7.51 (s, 1H), 8.01 (br, 1H, Ar–***H***), 8.26 (s, 1H, Ar–*H*). ^{13}C NMR (400 MHz, DMSO-d_6), δ 10.66, 30.46, 39.91 (–C attached to hydroxyl methyl) (merged in DMSO moisture), 62.48 (–***C***(CH_2)$_2$), 92.27 (C7 carbon), 103.36, 112.20, 117.34 (–*C*═*C*), and 151.85, 156.77, 157.81 (Ar–***C***). MS (ESI): m/z = 374.5 (M + H)$^+$.

8h (*E*-Isomer): Yield: 160 mg (38%). ^{1}H-NMR (400 MHz, DMSO-d_6) δ 1.51 (s, 2H, cyclopropyl CH_2), 3.50–3.44 (m, 4H (C***H***$_2$)$_2$), 4.70 (s, 2H), 7.65–7.64 (t, J = 4 Hz, 1H, Ar–***H***), 8.25 (s, 1H, Ar–*H*). ^{13}C NMR (400 MHz, DMSO-d_6), δ 14.56, 28.34, 39.92 (–C attached to hydroxyl methyl) (merged in DMSO moisture), 62.61 (–***C***(CH_2)$_2$), 92.44 (C7 carbon), 103.19, 111.90, 117.58 (–*C*═*C*), and 152.46, 156.43, 157.66 (Ar–***C***). MS (ESI): m/z = 374.5 (M + H)$^+$.

3.2.9. (2-((4-amino-1*H*-pyrazolo[3,4-*d*] pyrimidin-1-yl) methylene) cyclopropane-1,1-diyl) dimethanol (10a): compound 10a was obtained from (2-bromo-2-(bromomethyl) cyclopropane-1,1-diyl) bis(methylene) diacetate fallowed by deacetylation. *Z*-Isomer is a yellow solid and *E*-Isomer is a yellow solid. 10a (*E*-Isomer): Yield: 150 mg (54%). ^{1}H-NMR (400 MHz, DMSO-d_6) δ 1.49 (s, 2H, cyclopropyl CH_2), 3.51–3.45 (m, 4H, –C(C***H***$_2$)), 4.72 (s, 2H, O***H***), 7.70 (s, 1H), 7.93 (br, 1H, Ar–***H***), 8.22 (s, 1H, Ar–*H*).^{13}C NMR (400 MHz, DMSO-d_6), δ 11.06, 30.56, 39.92 (–C attached to hydroxyl methyl) (merged in DMSO moisture), 62.66 (–***C***(CH_2)$_2$), 100.21, 112.69, 116.50 (C7 carbon), 134.14 (–*C*═*C*), and 151.88, 156.88, 158.24 (Ar–***C***). MS (ESI): m/z = 248.5 (M + H)$^+$.

10a (*Z*-Isomer): Yield: 145 mg (52%). FT-IR (KBr): $\nu_{(-O-H)}$: 3183 cm^{-1}; $\nu_{(-C-H)}$: 2865 cm^{-1}; $\nu_{(-N-H \text{ bending})}$: 1665 cm^{-1}; $\nu_{(-C=C, \text{ aromatic})}$: 1565 cm^{-1}; $\nu_{(-C-O)}$: 984 cm^{-1}; $\nu_{(-C-O)}$: 1032 cm^{-1}; $\nu_{(-C-N)}$: 1291 cm^{-1}. ^{1}H-NMR (400 MHz, DMSO-d_6) δ 1.40 (s, 2H, cyclopropyl CH_2), 3.52–3.48 (m, 2H (C***H***$_2$)$_2$), 3.65–3.61 (m, 2H (C***H***$_2$)$_2$), 4.87 (s, 2H), 7.58 (s, 1H, Ar–***H***), 8.03 (br, 1H), 8.24 (s, 2H, Ar–*H*). ^{13}C NMR (400 MHz, DMSO-d_6), δ 11.06, 30.56, 39.92 (–C attached to hydroxyl methyl) (merged in DMSO moisture), 62.66 (–***C***(CH_2)$_2$), 100.21, 112.69, 116.50 (C7 carbon), 134.14 (–*C*═*C*), and 151.88, 156.88, 158.24 (Ar–***C***). MS (ESI): m/z = 248.5 (M + H)$^+$.

3.2.10. (2-((4-amino-3-iodo-1*H*-pyrazolo[3,4-*d*]pyrimidin-1-yl)methylene)cyclopropane-1,1-diyl)dimethanol (10b): compound 10b was obtained from (2-bromo-2-(bromomethyl) cyclopropane-1,1-diyl) bis(methylene) diacetate followed by deacetylation. *Z*-Isomer is an off-white solid and *E*-Isomer is an off-white solid. 10b (*Z*-Isomer): Yield: 180 mg (43%). ^{1}H-NMR (400 MHz, DMSO-d_6) δ 1.42 (s, 2H, cyclopropyl CH_2), 3.50–3.47 (d, J = 12.0 Hz, 2H, –C(C***H***$_2$)), 3.68–3.66 (d, J = 8.0 Hz, 2H, –C(C***H***$_2$)), 4.70 (s, 2H, O***H***), 6.80 (br, 1H, Ar–***H***), 7.51 (s, 1H), 8.26 (s, 1H, Ar–*H*).^{13}C NMR (400 MHz, DMSO-d_6), δ 10.66, 30.46, 39.92 (–C attached to hydroxyl methyl) (merged in DMSO moisture), 62.48 (–***C***(CH_2)$_2$), 92.75 (C7 carbon), 103.36, 112.20, 117.34 (–*C*═*C*), and 151.85, 156.77, 157.81 (Ar–***C***). FT-IR (KBr): $\nu_{(-O-H)}$: 3232 cm^{-1}; $\nu_{(-C-H)}$: 2871 cm^{-1}; $\nu_{(-N-H \text{ bending})}$: 1633 cm^{-1}; $\nu_{(-C=C, \text{ aromatic})}$: 1564 cm^{-1}; $\nu_{(-C-O)}$: 1021 cm^{-1}; $\nu_{(-C-N)}$: 1270 cm^{-1}; $\nu_{(-C-I)}$: 647 cm^{-1}. MS (ESI): m/z = 374.5 (M + H)$^+$.

10b (*E*-Isomer): Yield: 190 mg (45%). ^{1}H-NMR (400 MHz, DMSO-d_6) δ 1.51 (s, 2H, cyclopropyl CH_2), 3.52–3.44 (m, 4H (C***H***$_2$)$_2$), 4.70 (s, 2H), 7.65–7.64 (t, J = 4.0 Hz, 1H, Ar–***H***), 8.25 (s, 2H, Ar–*H*). ^{13}C NMR (400 MHz, DMSO-d_6), δ 14.56, 28.34, 39.92 (–C attached to hydroxyl methyl) (merged in DMSO moisture), 62.61 (–***C***(CH_2)$_2$), 92.44 (C7 carbon), 103.19, 111.90, 117.58 (–*C*═*C*), and 152.46, 156.43, 157.66 (Ar–***C***). MS (ESI): m/z = 374.5 (M + H)$^+$.

3.2.11. (2-((4-amino-3-(4-phenoxyphenyl)-1*H*-pyrazolo[3,4-*d*] pyrimidin-1-yl) methylene) cyclopropane-1,1-diyl) dimethanol (10c): compound 10c was obtained from (2-bromo-2-(bromomethyl) cyclopropane-1,1-diyl) bis(methylene) diacetate followed by deacetylation. *Z*-Isomer is an off-white solid and *E*-Isomer is an off-white solid. 10c (*Z*-Isomer): Yield: 200 mg (43%). ^{1}H-NMR (400 MHz, DMSO-d_6) δ 1.44 (s, 2H, cyclopropyl CH_2), 3.54–3.52 (d, J = 8.0 Hz, 2H, –C(C***H***$_2$)), 3.69–3.66 (d, J = 12.0 Hz, 2H, –C(C***H***$_2$)), 4.88 (s, 2H, O***H***), 7.23–7.14 (m, 15H, Ar–***H***), 7.48–7.43 (m, 2H), 7.71–7.69 (t, J = 8.0 Hz, 3H), 8.32 (s, 1H, Ar–*H*). ^{13}C NMR (400 MHz, DMSO-d_6), δ 11.03, 30.04, 39.92 (–C attached to hydroxyl methyl) (merged in DMSO moisture), 62.70 (–***C***(CH_2)$_2$), 79.17, 92.13, 112.27, 116.58, 118.92, 124.01, 126.74, 130.00 (–*C*═*C*), and 145.14 (C7 carbon), 152.99, 155.98, 156.65, 157.72, 158.33 (Ar–***C***). FT-IR (KBr): $\nu_{(-C-O-C)}$: 1243 cm^{-1}; $\nu_{(-O-H)}$: 3060 cm^{-1}; $\nu_{(-C-H)}$: 2039 cm^{-1}; $\nu_{(-N-H \text{ bending})}$: 1649 cm^{-1}; $\nu_{(-C=C, \text{ aromatic})}$: 1565 cm^{-1}; $\nu_{(-C-OH)}$: 1039 cm−1; $\nu_{(-C-N)}$: 1243 cm^{-1}. MS (ESI): m/z = 416.7 (M + H)$^+$.

10c (*E*-Isomer): Yield: 190 mg (41%). ^{1}H-NMR (400 MHz, DMSO-d_6) δ 1.52 (s, 2H, cyclopropyl CH_2), 3.51–3.47 (m, 4H (C***H***$_2$)$_2$), 4.72 (s, 2H), 7.21–7.13 (m, 5H), 7.46–7.44 (t, J = 8.0 Hz, 2H, Ar–***H***), 7.71–7.69 (d, J = 8.0 Hz, 2H), 7.79 (s, 1H), 8.30 (s, 2H,

 © 2024 The Author(s). Published by the Royal Society of Chemistry

Open Access Article. Published on 21 March 2024. Downloaded on 2/13/2026 12:19:14 PM. This article is licensed under a Creative Commons Attribution-NonCommercial 3.0 Unported Licence.

Ar–*H*). ^{13}C NMR (400 MHz, DMSO-d_6), δ 14.68, 28.31, 39.92 (–C attached to hydroxyl methyl) (merged in DMSO moisture), 62.74 (–***C***$(CH_2)_2$), 97.53, 112.20, 117.03, 119.03, 123.84, 127.51, 130.13 (–*C*=*C*), and 144.85 (C7 carbon), 153.56, 156.17, 156.24, 157.38, 158.11 (Ar–***C***). MS (ESI): $m/z = 416.7$ $(M + H)^+$.

3.3 α-Glucosidase inhibitory assay

The α-glucosidase inhibitory activity was assessed using the method described by Pistia Brueggeman and Hollingsworth, 2001,[47] with minor adjustments. Plant extracts, in volumes of 50 μL, were incubated with different concentrations ranging from 12.5 to 400 μg mL^{-1}. The incubation was carried out with 10 μL of α-glucosidase (maltase) enzyme solution (1 U mL^{-1}) for 20 minutes at a temperature of 37 °C. Additionally, 125 μL of 0.1 M phosphate buffer (pH 6.8) was added. Following 20 minutes, the reaction was initiated by adding 20 μL of 1 M pNPG (substrate), and the resulting mixture was allowed to incubate for 30 minutes. The reaction was halted by introducing 0.1 N of Na_2CO_3 (50 μL), and the ultimate absorbance was quantified at 405 nm. Acarbose was employed as a positive control, with doses ranging from 12.5 to 400 μg mL^{-1}. Enzyme activity was calculated as:

$$(OD_{blank} - OD_{sample})/OD_{blank} \times 100$$

A single unit of the enzyme can be precisely defined as the quantity of α-glucosidase enzyme necessary to produce one micromole of the product (*p*-nitrophenol) from the substrate (*p*-nitrophenyl-α-D-glucopyranoside) within one minute. The IC_{50}, which is the concentration needed to inhibit 50% of the enzyme activity, was determined by fitting a regression equation to a plot of concentration (ranging from 12.5–400 μg mL^{-1}) on the *x*-axis and % inhibition on the *y*-axis for various extracts and fractions.[48]

3.4 Antimicrobial activity

The agar well diffusion method was employed to determine the antibacterial activity.[49,50] The antibacterial efficacy of the synthesized compounds was assessed against four bacterial strains that included two Gram-positive bacteria, *Staphylococcus epidermis* (MTCC 2044), *Bacillus cereus* (MTCC2128) (Gram-positive) and two Gram-negative bacteria, *Escherichia coli* (MTCC2412), *Klebsiella pneumonia* (MTCC 2451). Different test compounds were introduced to wells perforated on an agar surface, with each well containing a concentration of 1 mg mL^{-1}. The bacterial strains were cultured in sterilized Mueller Hinton Broth (MHB) and incubated for 18 hours at 37 °C. The radius of the inhibition zone (RIZ) surrounding each well was measured in millimetres to assess the antibacterial activity. The experiments were conducted in duplicate. *Aspergillus niger* was utilized to assess the antifungal activity of the compounds. The fungal cultures were plated using the selective media known as Potato Dextrose Agar. The plates were subjected to incubation at a temperature of 37 °C for a duration ranging from 72 to 96 hours. Following this, the plates were checked for the zone of inhibition.

3.5 Swiss ADME

3.5.1. Evaluation of physico-chemical properties. The process of generating SMILES representations for all the designed compounds has been successfully concluded. The SMILES representations of the compounds were entered into SwissADME, an online tool freely available on the web (**http://www.swissadme.ch/index.php**),[34,51] along with their respective molecular codes. After the submission process is finished, the programme includes a "run" button feature that aids in the computation of the parameters. The gathered results were obtained in both PDF and CSV formats and subsequently underwent data analysis.

3.5.2. Molecular docking. The utilization of molecular docking facilitates the prediction of the optimal orientation of binding to the target protein, particularly when the ligand, which serves as the target, forms a stable complex with other possible ligands. Docking is a valuable technique for examining the molecular-level interaction between a protein and a ligand.

3.5.3. UCSF Chimera. UCSF Chimaera is commonly employed by structural biologists, biomedical researchers, and other professionals in the domains of bioinformatics and drug discovery to enhance their understanding of molecular structure and function. Chimaera is a versatile software application that facilitates the interactive visualization and analysis of molecular structures. It enables users to gain a deeper understanding of associated data, such as sequence alignments, density maps, supra-molecular assemblies, trajectories, docking results, and information about conformational ensembles.[52]

3.5.4. AutoDock Vina. The automated nature of the molecular docking programmed AutoDock Vina is evident. Enhancement of the ligand's ability to interact with the three-dimensional conformation of the target protein is seen. AutoDock Vina is widely recognized as a prominent bio-informatics software tool utilized for computational docking purposes. AutoDock Vina is widely employed for a diverse range of docking methodologies, encompassing site-specific docking, blind docking, and protein-ligand docking, among others. AutoDock Vina, also known as AutoDock Tools, provides support for structural alterations to both proteins and ligands, in addition to its docking capabilities. By employing this methodology, it becomes possible to evaluate molecular libraries of varying sizes. The provided information encompasses the values of root mean square deviation (RMSD), binding energy, and the number of hydrogen bonds (H-bonds) at position 44. A grid box for ITK with the dimensions *X*: 21, *Y*: −7.4, *Z*: 24.2 Å and the size of the grid box-21 × 21 × 21, was identified as the protein target docking site and the best molecular interacting compounds were observed.[53]

4 Conclusion

Individuals with diabetes are susceptible to numerous extra diseases due to a compromised immune system. Carbocyclic nucleosides possessing antibacterial and anti-inflammatory characteristics may offer significant advantages in the

Open Access Article. Published on 21 March 2024. Downloaded on 2/13/2026 12:19:14 PM. This article is licensed under a Creative Commons Attribution-NonCommercial 3.0 Unported Licence.

prevention of recurring infections and the facilitation of wound healing in patients with diabetes. Our research aimed to evaluate the α-glucosidase inhibitory activity of synthetic substances and their viability as therapeutic agents for the treatment of diabetes. *Staphylococcus* (a Gram-positive bacteria) and *Klebsiella* (a Gram-negative bacteria) were used as test organisms for antimicrobial activity, and the results showed that none of the chemicals examined showed any antimicrobial action. Compound **10b** (*Z*-Isomer) was shown to inhibit the growth of the Gram-positive bacterium *Bacillus cereus*. At 100 μl, the compound showed a peak inhibitory effect of 2.2 ± 0.25 mm. Inhibitory concentrations of **10a** (*Z*-Isomer) against the Gram-negative bacteria *Escherichia coli* were determined to be 75 μl (0.9 ± 0.05 mm) and 100 μl (1.2 ± 0.15 mm), respectively. There was no evidence of anti-fungal efficacy. Although the antibacterial properties of carbocyclic nucleosides show potential, additional investigation is required to clarify their modes of operation and assess their effectiveness and safety in diabetic individuals. The IC_{50} values of **8b** (*E*-Isomer) and **10a** (*E*-Isomer) were 43.292 nmol and 48.638 nmol, respectively, indicating that these two compounds are promising. Docking energies of 10.3 kcal mol^{-1} for compound **10a** (*E*-Isomer) and −9.4 kcal mol^{-1} for compound **8b** (*E*-Isomer) stood out among the produced compounds. Additional investigation is required to comprehensively comprehend the processes by which carbocyclic nucleosides function, the range of their effectiveness, and their clinical usefulness in the treatment of diabetes.

Ethical statement

This article does not contain any studies with animals performed by any of the authors.

Consent for publication

We authorize you to publish the article without any conflict.

Data availability

All data generated or analysed during this study are included in this published article and its ESI† files.

Author contributions

Mrs Kalyani Mallidi: investigation, formal analysis, methodology, and writing – original draft. Prof. Rambabu Gundla: validation, project administration and supervision. Dr Parameshwar Makam: conceptualisation, software, and writing – original draft. Dr Naresh Kumar Katari: data curation, and writing – review & editing. Prof. Sreekantha Babu Jonnalagadda: visualization, resources, and funding acquisition.

Conflicts of interest

The authors declare that they have no competing interests/competing interests.

Acknowledgements

The authors wish to thank the management of GITAM for the support and facilities.

Notes and references

1 L. The, *Lancet*, 2017, **389**, 2163–2262.
2 O. A. Ojo, H. S. Ibrahim, D. E. Rotimi, A. D. Ogunlakin and A. B. Ojo, *Med. Nov. Technol. Devices*, 2023, **19**, 100247.
3 C. J. Bailey and C. Day, *Br. Med. Bull.*, 2018, **126**(1), 123–137.
4 L. A. DiMeglio, C. Evans-Molina and R. A. Oram, *Lancet*, 2018, **391**, 2449–2462.
5 A. A. S. Akil, E. Yassin, A. Al-Maraghi, E. Aliyev, K. Al-Malki and K. A. Fakhro, *J. Transl. Med.*, 2021, **19**(1), 137.
6 K. J. Rotenberg, C. Bharathi and H. Davies, *Eat. Behav.*, 2017, **26**, 167–170.
7 C. Langenberg and L. A. Lotta, *Lancet*, 2018, **391**, 2463–2474.
8 I. Kyrou, C. Tsigos, C. Mavrogianni, G. Cardon, V. Van Stappen, J. Latomme, J. Kivelä, K. Wikström, K. Tsochev, A. Nanasi, C. Semanova, R. Mateo-Gallego, I. Lamiquiz-Moneo, G. Dafoulas, P. Timpel, P. E. H. Schwarz, V. Iotova, T. Tankova, K. Makrilakis, Y. Manios, J. Lindström, P. Schwarz, L. Annemans, I. Garamendi, M. Kontogianni, O. Androutsos, K. Tsoutsoulopoulou, C. Katsarou, E. Karaglani, I. Qira, E. Skoufas, K. Maragkopoulou, A. Tsiafitsa, I. Sotiropoulou, M. Tsolakos, E. Argyri, M. Nikolaou, E.-A. Vampouli, C. Filippou, K. Gatsiou, E. Dimitriadis, T. Laatikainen, P. Valve, E. Levälahti, E. Virtanen, R. Willems, I. Panchyrz, M. Holland, S. Liatis, C.-P. Lambrinou, A. Giannopoulou, L. Tsirigoti, E. Fappa, C. Anastasiou, K. Zachari, L. Rabemananjara, M. S. de Sabata, W. Ko, L. Moreno, F. Civeira, G. Bueno, P. De Miguel-Etayo, E. M. Gonzalez-Gil, M. I. Mesana, G. Vicente-Rodriguez, G. Rodriguez, L. Baila-Rueda, A. Cenarro, E. Jarauta, N. Usheva, N. Chakarova, S. Galcheva, R. Dimova, Y. Bocheva, Z. Radkova, V. Marinova, Y. Bazdarska, T. Stefanova, I. Rurik, T. Ungvari, Z. Jancsó, A. Nánási, L. Kolozsvári, C. Semánova, R. Martinez, M. Tong, K. Joutsenniemi and K. Wendel-Mitoraj, *BMC Endocr. Disord.*, 2020, **20**(1), 134.
9 S. D. Ray, A. Hussain, A. Niha, M. Krmic, A. Jalshgrari, D. Genis and J. Reji, Anti Diabetic Agents, in *Encyclopedia of Toxicology*, ed. P. Wexler, Academic Press, Oxford, 4th edn, 2024, pp. 573–589.
10 C. M. Khoo, *Diabetes Mellitus Treatment*, ed. S.R. Quah, Academic Press, Oxford, 2017, pp. 288–293.
11 A. Berbudi, N. Rahmadika, A. I. Tjahjadi and R. Ruslami, *Curr. Diabetes Rev.*, 2020, **16**(5), 442–449.
12 G. Daryabor, M. R. Atashzar, D. Kabelitz, S. Meri and K. Kalantar, *Front. Immunol.*, 2020, 11.
13 J. Chávez-Reyes, C. E. Escárcega-González, E. Chavira-Suárez, A. León-Buitimea, P. Vázquez-León, J. R. Morones-Ramírez, C. M. Villalón, A. Quintanar-Stephano and B. A. Marichal-Cancino, *Public Health Front.*, 2021, **9**, 559595.
14 J. Casqueiro and C. Alves, *Indian J. Endocrinol. Metab.*, 2012, **1**(1), 2230–8210.

© 2024 The Author(s). Published by the Royal Society of Chemistry

Open Access Article. Published on 21 March 2024. Downloaded on 2/13/2026 12:19:14 PM. This article is licensed under a Creative Commons Attribution-NonCommercial 3.0 Unported Licence.

15 S. Erener, *Mol. Metab.*, 2020, **39**, 101044.
16 B. J. Eckhardt and R. M. Gulick, *Infect. Dis.*, 2017, 1293–1308.
17 P. D. Kennewell, *Compr. Med. Chem. II*, 2007, **1**, 97–249.
18 S. Rachakonda and L. Cartee, *Curr. Med. Chem.*, 2004, **11**(6), 775–793.
19 D. Xia, F. Wang and M. J. Parmely, *Biochem. Pharmacol.*, 2000, **60**(5), 717–727.
20 S. M. Daluge, S. S. Good, M. B. Faletto, W. H. Miller, M. H. St Clair, L. R. Boone, M. Tisdale, N. R. Parry, J. E. Reardon, R. E. Dornsife, D. R. Averett and T. A. Krenitsky, *Antimicrob. Agents Chemother.*, 1997, **41**(5), 1082–1093.
21 J. Huuskonen, D. J. Livingstone and D. T. Manallack, *SAR QSAR Environ. Res.*, 2008, **19**(3–4), 191–212.
22 M. Yazdanian, S. L. Glynn, J. L. Wright and A. Hawi, *Pharm. Res.*, 1998, **15**(9), 1490–1494.
23 P. Artursson, A.-L. Ungell and J.-E. Löfroth, *Pharm. Res.*, 1993, **10**(8), 1123–1129.
24 M. Sharifi and T. Ghafourian, *AAPS J.*, 2014, **16**(1), 65–78.
25 M. V. Varma, Y. Lai and A. F. El-Kattan, *Adv. Drug Delivery Rev.*, 2017, **116**, 92–99.
26 S. Struck, U. Schmidt, B. Gruening, I. S. Jaeger, J. Hossbach and R. Preissner, *Toxicity versus Potency: Elucidation of Toxicity Properties Discriminating between Toxins, Drugs, and Natural Compounds*, Imperial College Press, 2008, pp. 231–242.
27 C. A. Lipinski, F. Lombardo, B. W. Dominy and P. J. Feeney, *Adv. Drug Delivery Rev.*, 1997, **23**(1–3), 3–25.
28 C. A. Lipinski, F. Lombardo, B. W. Dominy and P. J. Feeney, *Adv. Drug Delivery Rev.*, 2001, **46**(1–3), 3–26.
29 I. Kola and J. Landis, *Nat. Rev. Drug Discovery*, 2004, **3**(8), 711–716.
30 D. F. Veber, S. R. Johnson, H.-Y. Cheng, B. R. Smith, K. W. Ward and K. D. Kopple, *J. Med. Chem.*, 2002, **45**(12), 2615–2623.
31 P. D. Leeson and A. M. Davis, *J. Med. Chem.*, 2004, **47**(25), 6338–6348.
32 M. P. Gleeson, A. Hersey, D. Montanari and J. Overington, *Nat. Rev. Drug Discovery*, 2011, **10**(3), 197–208.
33 S. Khojasteh, H. Wong and C. C. A. Hop, *Drug Metabolism and Pharmacokinetics Quick Guide*, Springer, New York, 2011, pp. 165–181.
34 A. Daina, O. Michielin and V. Zoete, *Sci. Rep.*, 2017, **7**(1), 42717.
35 M. Hocek, P. Nauš, R. Pohl, I. Votruba, P. A. Furman, P. M. Tharnish and M. J. Otto, *J. Med. Chem.*, 2005, **48**(18), 5869–5873.
36 L. A. Agrofoglio, I. Gillaizeau and Y. Saito, *Chem. Rev.*, 2003, **103**(5), 1875–1916.
37 Y.-L. Qiu, M. B. Ksebati, R. G. Ptak, B. Y. Fan, J. M. Breitenbach, J.-S. Lin, Y.-C. Cheng, E. R. Kern, J. C. Drach and J. Zemlicka, *J. Med. Chem.*, 1998, **41**(1), 10–23.
38 R. J. Rybak, J. Zemlicka, Y. L. Qiu, C. B. Hartline and E. R. Kern, *Antiviral Res.*, 1999, **43**(3), 175–188.
39 R. J. Rybak, C. B. Hartline, Y. L. Qiu, J. Zemlicka, E. Harden, G. Marshall, J. P. Sommadossi and E. R. Kern, *Antimicrob. Agents Chemother.*, 2000, **44**(6), 1506–1511.
40 Z. Yan, E. R. Kern, E. Gullen, Y. C. Cheng, J. C. Drach and J. Zemlicka, *J. Med. Chem.*, 2005, **48**(1), 91–99.
41 D. Ramesh, B. G. Vijayakumar and T. Kannan, *ChemMedChem*, 2021, **16**(9), 1403–1419.
42 M. Kasula, M. Toyama, R. Samunuri, F. Rozy, M. Yadav, C. Bal, A. K. Jha, M. Baba and A. Sharon, *Bioorg. Med. Chem. Lett.*, 2016, **26**(16), 3945–3949.
43 R. Samunuri, A. K. Jha and C. Bal, *Nucleosides, Nucleotides Nucleic Acids*, 2019, **38**(6), 391–399.
44 H. T. Nguyen, T. T. Nguyen, T. H. Duong, N. M. Tran, C. H. Nguyen, T. H. Nguyen and J. Sichaem, *Molecules*, 2022, **27**(8), 2574.
45 C. T. Meyer, D. J. Wooten, B. B. Paudel, J. Bauer, K. N. Hardeman, D. Westover, C. M. Lovly, L. A. Harris, D. R. Tyson and V. Quaranta, *Cell Syst.*, 2019, **8**(2), 97–108.
46 V. M. Patil, K. N. Tilekar, N. M. Upadhyay and C. S. Ramaa, *ChemistrySelect*, 2022, **7**(1), e202103848.
47 G. Pistia-Brueggeman and R. I. Hollingsworth, *Tetrahedron*, 2001, **57**(42), 8773–8778.
48 A. Bhatia, B. Singh, R. Arora and S. Arora, *BMC Complementary Altern. Med.*, 2019, **19**(1), 74.
49 S. Magaldi, S. Mata-Essayag and C. Hartung de Capriles, *Int. J. Infect. Dis.*, 2004, **8**, 39–45.
50 C. Valgas, S. M. De Souza, E. F. Smânia and A. Smânia Jr, *Braz. J. Microbiol.*, 2007, **38**, 369–380.
51 B. Bakchi, A. D. Krishna, E. Sreecharan, V. B. J. Ganesh, M. Niharika, S. Maharshi, S. B. Puttagunta, D. K. Sigalapalli, R. R. Bhandare and A. B. Shaik, *J. Mol. Struct.*, 2022, **1259**, 132712.
52 E. F. Pettersen, T. D. Goddard, C. C. Huang, G. S. Couch, D. M. Greenblatt, E. C. Meng and T. E. Ferrin, *J. Comput. Chem.*, 2004, **25**(13), 1605–1612.
53 O. Trott and A. J. Olson, *J. Comput. Chem.*, 2010, **31**(2), 455–461.

© 2024 The Author(s). Published by the Royal Society of Chemistry